

Possible scenarios for soft and semi-hard components structure in
central hadron–hadron collisions in the TeV region:
pseudo-rapidity intervals.

A. Giovannini

*Dipartimento di Fisica Teorica and I.N.F.N – sezione di Torino
via P. Giuria 1, 10124 Torino, Italy*

R. Ugoccioni

*CENTRA and Departamento de Física (I.S.T.),
Av. Rovisco Pais, 1096 Lisboa codex, Portugal*

Abstract

Continuing previous work on collective variables properties in full phase space in hadron-hadron collisions in the TeV region our investigation is extended to multiplicity distributions and clan structure analysis in pseudo-rapidity intervals. Total multiplicity distributions (MDs) are considered also here as the weighted superposition of soft and semi-hard components, and described by Pascal(NB)MD. The soft component is characterised by KNO and Feynman scaling behaviour in all scenarios which differ in the semi-hard component properties only. In fact, the semi-hard component has been supposed to satisfy, in scenario 1, KNO and Feynman scaling behaviour and to violate it strongly in scenario 2. A third possibility has been explored: it is a QCD inspired scenario and leads to expectations intermediate between the just mentioned two. The semi-hard component structure becomes dominant in the TeV energy domain, a huge mini-jet production is indeed the main phenomenon in this region. In addition a new species of clans is generated suggesting a phase transition in the clan production in scenarios 2 and 3. Our results can be compared with TEVATRON and LHC experimental data when available.

1 Introduction

In the first paper of this series [1] (from now on referred to as ‘I’), possible scenarios for collective variables properties in the TeV region have been examined in full phase space. Stated that shoulder structure in P_n vs. n and H_q vs. q oscillations can be interpreted for c.m. energies larger than 200 GeV as the effect of the weighted superposition of soft and semi-hard events, each class being described by a single Pascal (also known as negative binomial [1]) multiplicity distribution, (Pa(NB)MD)

$$P_n^{(\text{PaNB})}(\bar{n}, k) = \frac{k(k+1) \dots (k+n-1)}{n!} \frac{\bar{n}^n k^k}{(\bar{n} + k)^{n+k}} \quad (1)$$

our approach consisted in finding physically motivated extrapolations of the free parameters of the mentioned distributions starting from their known behaviour in the GeV energy region. This fact has led us to imagine firstly possible extreme scenarios in the TeV region which basically should fix upper and lower bounds to the allowed variation path of the average multiplicity \bar{n}_i and of the parameter k_i , which is linked to the dispersion D_i by

$$(D_i^2 - \bar{n}_i)/\bar{n}_i^2 = 1/k_i \quad (2)$$

Here i stands for ‘soft’ or ‘semi-hard’. Accordingly, in scenario 1 we assumed KNO scaling to be valid both for $P_{n,\text{soft}}$ and $P_{n,\text{semi-hard}}$ multiplicity distributions (MDs); consequently, k_{soft} and $k_{\text{semi-hard}}$ parameters were taken constant with energy. In scenario 2, KNO scaling is realized for the soft component only (k_{soft} constant with energy) and $1/k_{\text{semi-hard}}$ increases linearly in $\ln(\sqrt{s})$. Between these two quite extreme possibilities we proposed a third scenario, which in view of the chosen behaviour of the parameters of $P_{n,\text{semi-hard}}$ was called a QCD inspired scenario (the scenarios are described in greater detail in Section 3).

It is interesting to remark that data on MDs at 1.8 TeV c.m. energy (from the E735 experiment [2]), when compared with our predictions, are closer to scenario 2, characterised by a huge mini-jet production in the semi-hard component, but go beyond it showing an even wider MD: assuming these data will be confirmed, observed deviations from expectations of scenario 2 might very well indicate the onset in our framework of new substructures in the total MDs, which we suggested to interpret as probably due to a new species of mini-jets (see I). Our caution on this point was and is motivated by the fact that mentioned data on MDs in full phase space (f.p.s.) at lower c.m. energies show systematic differences with respect to UA5 data [3] on which is based our general scheme for defining scenarios 1 and 2. That’s the reason why we decided to maintain this scheme also for extending our previous work from f.p.s. to pseudo-rapidity intervals. When data of the E735 experiment will be consolidated it is indeed not a too hard job to adapt our approach to the new experimental framework.

2 P_n vs n behaviour in pseudo-rapidity intervals in the GeV and TeV energy domains

In going from full phase space (f.p.s.) to pseudo-rapidity (η) intervals, our main concern is to be consistent with the scenarios explored in f.p.s., and extend them.

In f.p.s., the quadratic growth (in $\ln \sqrt{s}$) of the total average multiplicity was attributed to the growing contribution of semi-hard events. Notice that semi-hard events are defined by the presence of mini-jets or jets in the final state, irrespectively of the pseudo-rapidity interval under consideration. It must be stressed that only after this classification of events has been carried out we look at phase space intervals: thus the description of the total MD, $P_n(\eta_c, \sqrt{s})$, in terms of a weighted superposition of two multiplicity distributions holds in η intervals with the same weighting factor as in f.p.s., namely α_{soft} , function of energy only and not of η_c (the η_c dependence comes from \bar{n} and k parameters), i.e.:

$$P_n(\eta_c, \sqrt{s}) = \alpha_{\text{soft}}(\sqrt{s}) P_n^{(\text{PaNB})}(\bar{n}_{\text{soft}}(\eta_c, \sqrt{s}), k_{\text{soft}}(\eta_c, \sqrt{s})) + (1 - \alpha_{\text{soft}}(\sqrt{s})) P_n^{(\text{PaNB})}(\bar{n}_{\text{semi-hard}}(\eta_c, \sqrt{s}), k_{\text{semi-hard}}(\eta_c, \sqrt{s})) \quad (3)$$

precisely as in eq. (I.2).

In this paper, we will be concerned with symmetric pseudo-rapidity intervals $[-\eta_c, \eta_c]$, with $1 \leq \eta_c \leq 3$. The joining of these intervals to f.p.s. is assumed to be smooth.

2.1 Average multiplicity in pseudo-rapidity intervals

In f.p.s. (see I, Section 2.1), it was assumed that each component has an average multiplicity which grows linearly with $\ln \sqrt{s}$:

$$\bar{n}_{\text{soft}}(\sqrt{s}) = -5.54 + 4.72 \ln(\sqrt{s}) \quad (\text{I.3})$$

$$\bar{n}_{\text{semi-hard}}(\sqrt{s}) \approx 2\bar{n}_{\text{soft}}(\sqrt{s}) \quad (\text{I.4.A})$$

Since the width of available phase space also grows linearly with $\ln \sqrt{s}$, we find that the simplest way to be consistent with our assumptions is to say that the single particle density must show an energy independent plateau around $\eta = 0$ which extends some units in each direction (a plateau of this size is found in experimental data at UA5 energies for the full distribution: its height increases with c.m. energy indicating violation of Feynman scaling.)

Numerically, we fix the height \bar{n}_0 of the soft and semi-hard plateaus again respecting the result of [4] in the investigation of UA5 data:

$$\bar{n}_{0,\text{soft}} \approx 2.45, \quad \bar{n}_{0,\text{semi-hard}} \approx 6.4 \quad (4)$$

and

$$\bar{n}_i(\eta_c) = 2\bar{n}_{0,i}\eta_c \quad (i = \text{soft, semi-hard}) \quad (5)$$

Accordingly, from eq. (3)

$$\bar{n}_{\text{total}}(\eta_c, \sqrt{s}) = \alpha_{\text{soft}}(\sqrt{s})\bar{n}_{\text{soft}}(\eta_c) + (1 - \alpha_{\text{soft}}(\sqrt{s}))\bar{n}_{\text{semi-hard}}(\eta_c) \quad (6)$$

where the last line follows from eq. (3). Notice that the semi-hard component is more than twice the soft component, and the value 2.45 for the soft component is compatible with low energy data (e.g., ISR data), where only the soft component is present.

There are no compelling physical reasons to assume that also the semi-hard component has an energy independent plateau. Indeed a logarithmic growth of the plateau with c.m. energy is compatible with a second possibility that was considered in I for the growth of $\bar{n}_{\text{semi-hard}}$:

$$\bar{n}_{\text{semi-hard}}(\sqrt{s}) \approx 2\bar{n}_{\text{soft}}(\sqrt{s}) + 0.1 \ln^2(\sqrt{s}) \quad (\text{I.4.B})$$

In the simplest approach where one neglects energy variations of $d\bar{n}/d\eta$ at the boundary of phase space, a parameterisation of the growth numerically compatible with eq. (I.4.B) is

$$\bar{n}_{0,\text{semi-hard}} \approx 6.3 + 0.07 \ln \sqrt{s} \quad (7)$$

the effect of which in the 1–20 TeV range is in complete agreement with f.p.s. Therefore we limit ourselves to showing figures only for the case of linear \bar{n}_{soft} , mentioning the differences in the text below when relevant. We postpone to future work the discussion of the case in which the particle density varies at the boundary of phase space.

2.2 Dispersion in pseudo-rapidity intervals

We now examine the width of the multiplicity distribution; to this end, we use the parameter k as defined in eq. (2). In particular, we have the following relation:

$$\bar{n}_{\text{total}}^2 \left(1 + \frac{1}{k_{\text{total}}}\right) = \alpha_{\text{soft}} \bar{n}_{\text{soft}}^2 \left(1 + \frac{1}{k_{\text{soft}}}\right) + (1 - \alpha_{\text{soft}}) \bar{n}_{\text{semi-hard}}^2 \left(1 + \frac{1}{k_{\text{semi-hard}}}\right) \quad (8)$$

obtained from eq.s (3) and (6) (for brevity, the dependence on η_c and \sqrt{s} has been omitted in this formula). The behaviour of k_{soft} and $k_{\text{semi-hard}}$ is indeed of great importance in our subsequent discussion for at least three reasons. Firstly, in view of k 's relationship with the two-particle correlation function $C_2(\eta_1, \eta_2; \sqrt{s})$, [5]:

$$k^{-1}(\eta_c; \sqrt{s}) = \frac{1}{\bar{n}^2(\eta_c; \sqrt{s})} \iint_{-\eta_c}^{\eta_c} C_2(\eta_1, \eta_2; \sqrt{s}) d\eta_1 d\eta_2 \quad (9)$$

k_{soft} and $k_{\text{semi-hard}}$ control two-particle correlation properties of the two components. Secondly, clan structure parameters, $\bar{N}_i(\eta_c, \sqrt{s})$ and $\bar{n}_{c,i}(\eta_c, \sqrt{s})$ ($i = \text{soft, semi-hard}$), are defined for each component in terms of \bar{n}_i and k_i as follows [5]:

$$\begin{aligned} \bar{N}_i(\eta_c, \sqrt{s}) &= k_i(\eta_c, \sqrt{s}) \ln \left(1 + \bar{n}_i(\eta_c)/k_i(\eta_c, \sqrt{s})\right); \\ \bar{n}_{c,i}(\eta_c, \sqrt{s}) &= \bar{n}_i(\eta_c)/\bar{N}_i(\eta_c, \sqrt{s}) \end{aligned} \quad (10)$$

It should be pointed out that the above definition is valid for a single Pa(NB)MD only: as explained in [1], clans cannot be defined for the total MD which, being the superposition of two (or possibly more) Pa(NB)MDs with in general different parameters, is not of Pa(NB)MD type. The third reason is a consequence of eq. (10), which allows us to interpret $1/k_i$ for a single Pa(NB)MD only:

$$k_i^{-1} = \frac{\text{P}_i(1; 2)}{\text{P}_i(2; 2)} \quad (11)$$

Table 1: Values of the parameters assumed in our extrapolations for $1/k = (D^2 - \bar{n})/\bar{n}^2$, for each component, for each rapidity interval examined and for f.p.s., too. For the soft one and for scenario 1, $1/k$ is energy independent and given in the table; in the other cases the relevant parameters are given.

interval	soft comp.	scenario 1	scenario 2	scenario 3
$ \eta \leq \eta_c$	k_{soft}^{-1}	$k_{\text{semi-hard}}^{-1}$	$k_{\text{total}}^{-1}(\eta_c, \sqrt{s}) = a + b \ln \sqrt{s}$	$k_{\text{semi-hard}}^{-1}(\eta_c, \sqrt{s}) = C + D/\sqrt{\ln(\sqrt{s}/10)}$
$\eta_c = 1$	0.294	0.217	$a = 0.02$ $b = 0.08$	$C = 0.97$ $D = -1.6$
$\eta_c = 2$	0.286	0.172	$a = -0.06$ $b = 0.08$	$C = 0.88$ $D = -1.5$
$\eta_c = 3$	0.250	0.156	$a = -0.12$ $b = 0.08$	$C = 0.72$ $D = -1.2$
f.p.s	0.143	0.077	$a = -0.082$ $b = 0.0512$	$C = 0.38$ $D = -0.42$

where $P_i(N; m)$ is the probability to have m particles belonging to N clans [6]. Therefore any assumption or result on the energy or pseudo-rapidity dependence of k_i has its counterpart in all above mentioned frameworks.

The soft component is taken to have $1/k$ constant with energy for each η interval, but variable with the width of the interval. In low energy experimental data, $1/k$ is not constant but KNO scaling holds: in view of the growing value of \bar{n} , KNO scaling implies at high energies that $1/k$ reaches a constant value, which we infer from the highest energy data point in reference [4]. For the actual numbers, see table 1; the behaviour of all the relevant Pa(NB)MD parameters is shown in Figures 1, 2 and 3. We notice that $1/k$ decreases slowly by increasing the width of the η interval: as the interval gets larger, there is less aggregation. Particles generated by new clans fill the growing interval faster than those generated by old clans. Accordingly the linear growth of the average number of clans \bar{N} is faster than the increase in the average number of particles per clan, \bar{n}_c . This behaviour also implies that, having clans a large extension in pseudo-rapidity, long range correlations become important.

In summary, for the soft component both \bar{n} and k are constant with energy: so are the clan parameters. \bar{n} , \bar{N} and \bar{n}_c all grow with η_c , while $1/k$ decreases.

3 The three scenarios in pseudo-rapidity intervals

For the semi-hard component, since in f.p.s. we devised three scenarios with a different variation of the dispersion of the multiplicity distribution with energy, we use the fact that low energy experimental results for the dispersion show the same energy behaviour in η intervals as in f.p.s., and extend the f.p.s. behaviour to pseudo-rapidity intervals.

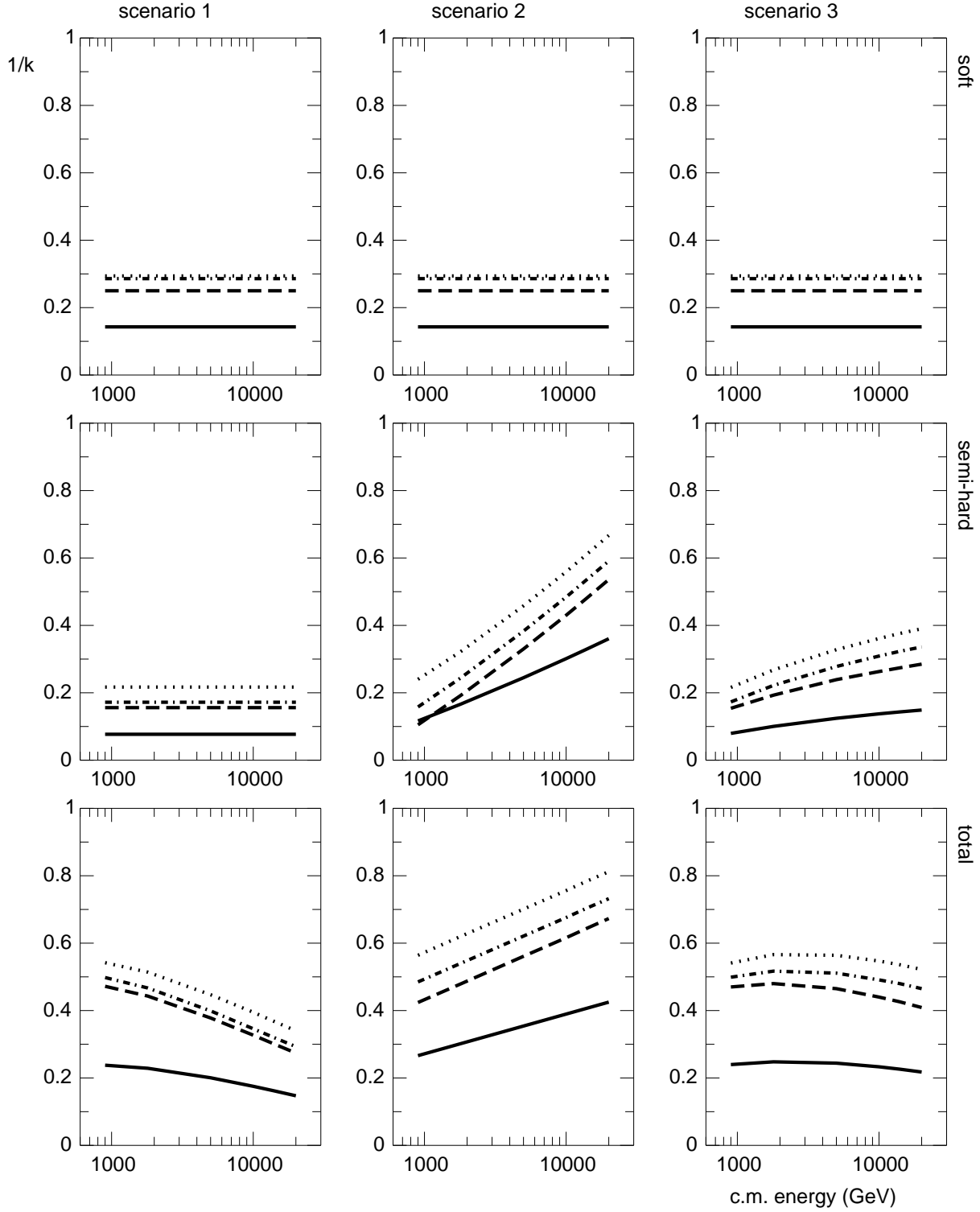


Figure 1: The Pa(NB)MD parameter $1/k$ is plotted against the c.m. energy for three rapidity intervals (dotted line: $\eta_c = 1$; dash-dotted line: $\eta_c = 2$; dashed line: $\eta_c = 3$) and for f.p.s. (solid line), for each scenario (in columns, from left to right: scenario 1, 2 and 3) and for each component (in rows, from top to bottom: soft, semi-hard, total distribution).

3.1 Scenario 1

The first scenario is characterized by a Feynman scaling and KNO scaling semi-hard component, just as for the soft component, but with different values for the parameters, see table 1 and the leftmost column of Figure 1: the average multiplicity is more than double, and $1/k$ is smaller, so that even with more particles there is less aggregation. In this case, the total distribution's k_{total} parameter is given by the superposition formula, Eq. (8).

It is interesting to notice in connection with this scenario that correlations increase due to the superposition of events of different type, both with smaller correlations, as

$$1/k_{\text{total}} > 1/k_{\text{soft}} > 1/k_{\text{semi-hard}} \quad (12)$$

This is an example of the situation examined in detail in [7]: these enhanced correlations are a consequence of the fluctuations in single particle densities (due to the superposition of events with different average multiplicity), superimposed to “genuine” two-particle correlations.

Furthermore, the behaviour of $1/k_{\text{total}}$ with energy is peculiar in that it first increases (up to about 1 TeV) then decreases: the maximum is rather wide, resulting in an accidental KNO scaling behaviour for c.m. energy $0.5 \lesssim \sqrt{s} \lesssim 1.8$ TeV.

The KNO scaling behaviour of the total MD is unexpected because although we are superimposing two KNO scaling distributions, we are doing it with an energy dependent weight parameter. Of course scaling behaviour is expected both at low energy (only the soft component is present) and at very high energy, because in this simple picture only the semi-hard component is present.

The energy independence of \bar{n} and k in fixed η intervals is contrasted with their energy dependence in f.p.s. in terms of clan parameters in the leftmost column in Figures 2 and 3.

The effect of a quadratic growth of $\bar{n}_{\text{semi-hard}}$ with energy is to increase slightly (around 10%) the value of $1/k_{\text{total}}$, compatibly with what we have seen in f.p.s.

3.2 Scenario 2

For the second scenario we choose to violate KNO scaling by making $1/k_{\text{total}}$ continue to grow with energy as it does up to UA5 energies with a linear behaviour in $\ln \sqrt{s}$ as given in table 1, where the parameters a and b have been fitted to experimental data from ISR to UA5. Notice that it appears that the best slope b is the same for each interval. $1/k_{\text{semi-hard}}$ is then obtained using eq. (8): it also grows approximately linearly with c.m. energy, and decreases rapidly as η_c increases (see Figure 1, central column). In particular, above 1 TeV, $1/k_{\text{semi-hard}}$ becomes larger than $1/k_{\text{soft}}$: this implies that correlations are much larger in the semi-hard events than in the soft events; because in both cases $k < \bar{n}$, this is probably due again to fluctuations in single particle distribution (the semi-hard component has indeed larger fluctuations in multiplicity).

At the same time, the average number of clans is seen to decrease very rapidly with the energy for the semi-hard component, \bar{n}_c is seen to increase with energy; it also increases with η_c , and the increase is faster when the energy is higher (Figures 2 and 3.)

The effect of a quadratic growth of $\bar{n}_{\text{semi-hard}}$ with energy is to decrease slightly (less than 10%) the value of $1/k_{\text{semi-hard}}$, compatibly with what we have seen in f.p.s.

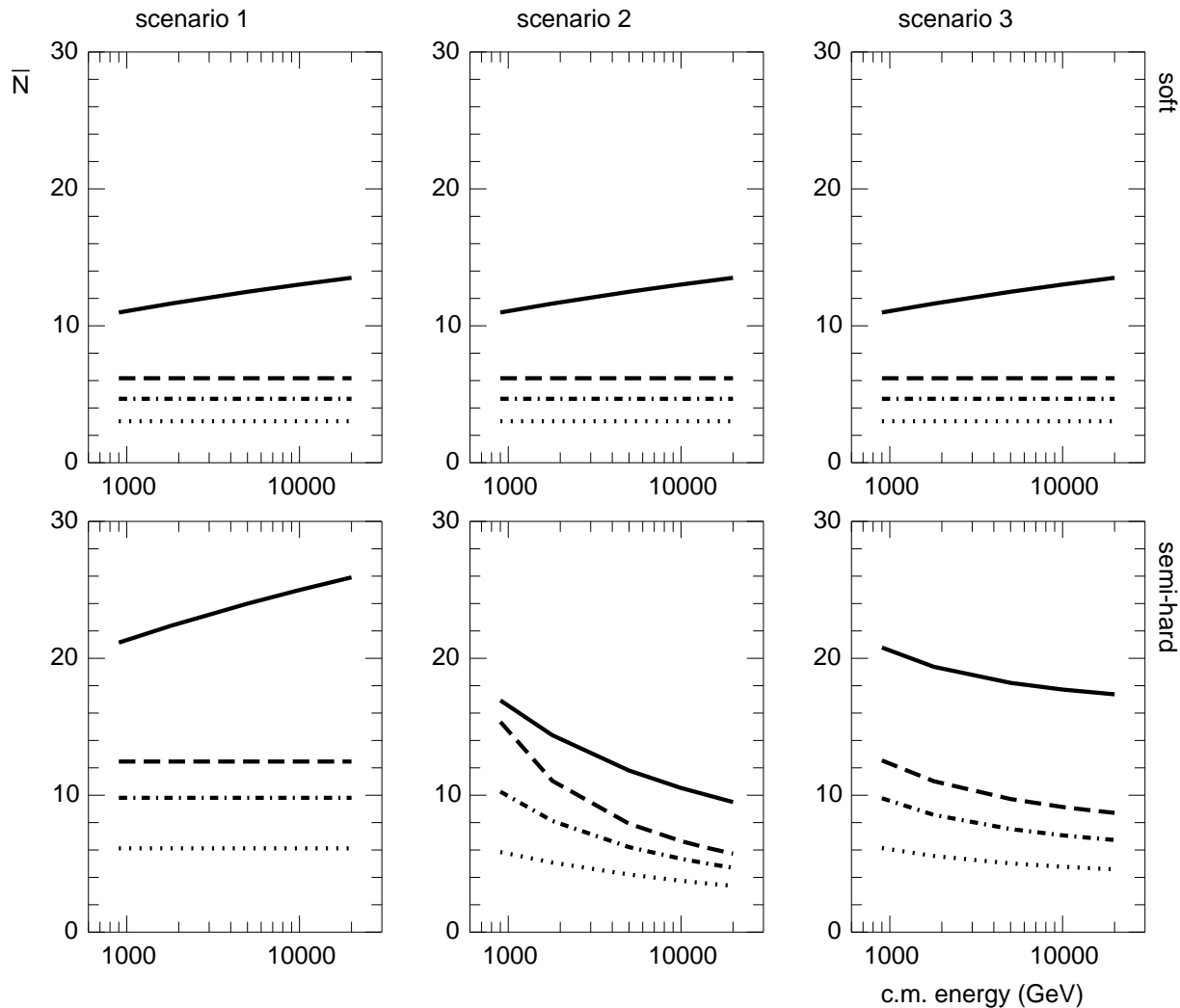


Figure 2: The average number of clans \bar{N} is plotted against the c.m. energy for three rapidity intervals (dotted line: $\eta_c = 1$; dash-dotted line: $\eta_c = 2$; dashed line: $\eta_c = 3$) and for f.p.s. (solid line), for each scenario (in columns, from left to right: scenario 1, 2 and 3) and for each component (in rows, from top to bottom: soft and semi-hard).

3.3 Scenario 3

In the third scenario we chose a QCD inspired shape, which has a behaviour which turns out to be intermediate between scenario 1 and 2: it starts growing with energy but asymptotically (well above the energy range we consider here) tends to a constant value:

$$\frac{1}{k_{\text{semi-hard}}} = C + \frac{D}{\sqrt{\ln(\sqrt{s}/10)}} \quad (13)$$

Again the values of the parameters for each interval are given in table 1: they were chosen to be compatible with the 900 GeV points [4] and to lead to an intermediate value of $1/k$. The general behaviour of the Pa(NB)MD parameters is shown in the rightmost column of Figures 1, 2 and 3.

While the behaviour of the parameters for the semi-hard component is qualitatively

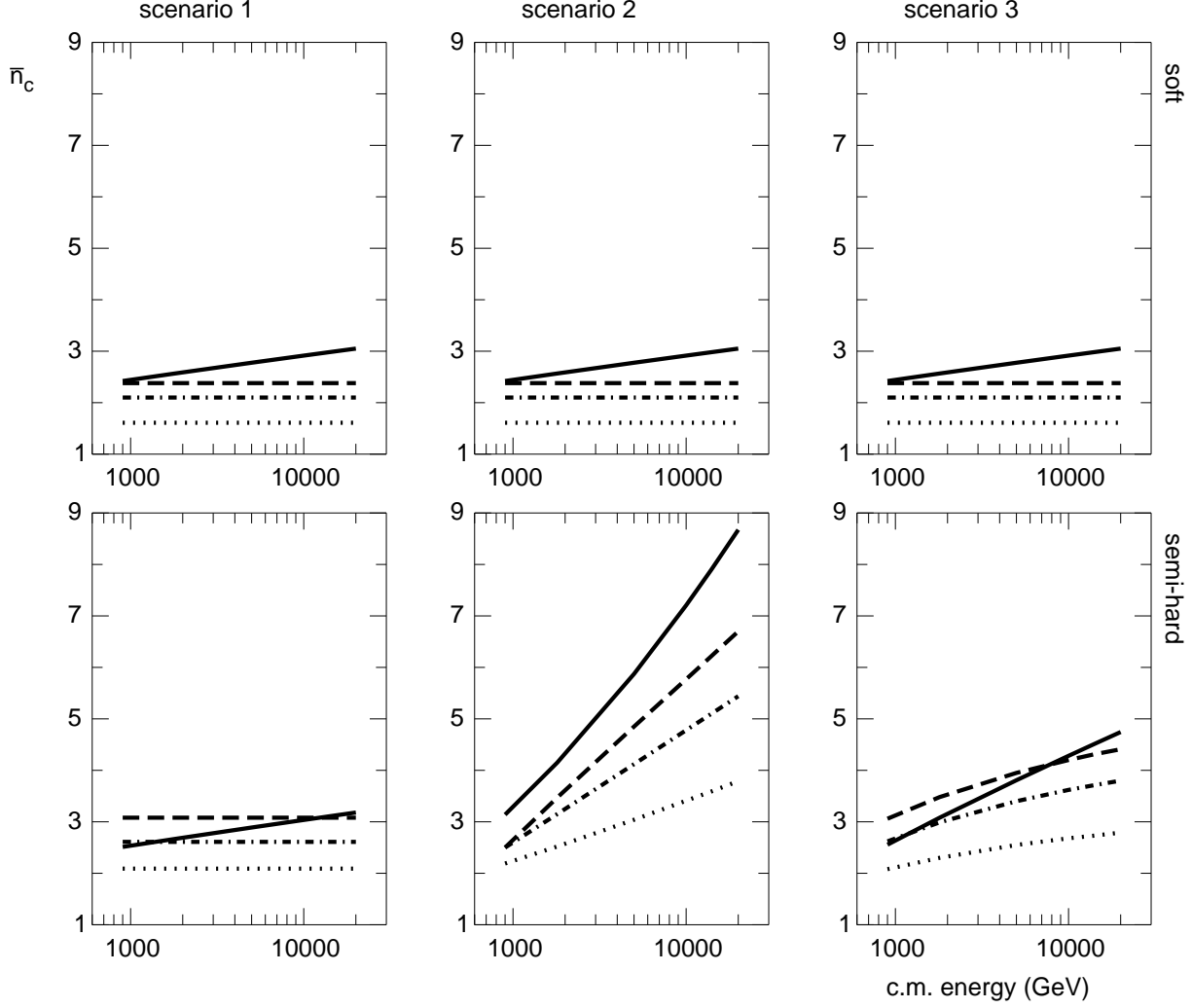


Figure 3: The average number of particles per clan, \bar{n}_c is plotted against the c.m. energy for three rapidity intervals (dotted line: $\eta_c = 1$; dash-dotted line: $\eta_c = 2$; dashed line: $\eta_c = 3$) and for f.p.s. (solid line), for each scenario (in columns, from left to right: scenario 1, 2 and 3) and for each component (in rows, from top to bottom: soft and semi-hard).

similar to that of scenario 2, the behaviour for the total MD is qualitatively similar to that of scenario 1. Indeed, the increase of $1/k$ for the semi-hard with c.m. energy is not as fast as in scenario 2, and $1/k$ is smaller in this case, so this leads, for the total distribution, to a broad maximum in the energy range 2-10 TeV, which implies KNO scaling. The decrease from the maximum is slower than in scenario 1, and this accidental KNO scaling appears at higher energies.

The effect of a quadratic growth of $\bar{n}_{\text{semi-hard}}$ with energy is to increase slightly (around 10%) the value of $1/k_{\text{total}}$, compatibly with what we have seen in f.p.s.

4 Comments on the three scenarios

It is quite clear that in scenario 1 both soft and semi-hard components show wide self-similarity regions [8]: the parameters k_{soft} and $k_{\text{semi-hard}}$ vary very little from one pseudo-rapidity interval to another. A quite strong point, which can easily be tested by using Pa(NB)MD with a fixed k (soft or semi-hard) parameter (determined by data in a small domain of rapidity space) as a “microscope”: by enlarging slowly the initial domain in rapidity one can explore up to which interval MDs are described by Pa(NB)MDs with the same initial k . This exercise will tell us that in that region two-particle correlations are dominant and that they vary according to the normalization $\bar{n}_{\text{semi-hard}}^2(\eta_c)$ only. It should also be noticed that the fact that k parameter is energy independent in a fixed rapidity interval and vary very little from one interval to another has important consequences on \bar{N}_{soft} and $\bar{N}_{\text{semi-hard}}$ (see Fig. 2): they do not vary with energy in a fixed rapidity interval and only very slowly by increasing the rapidity interval; their growth with energy in full phase space is due to the growth of the average number of particles with a constant k parameter.

In scenario 2 the soft component shows of course for all parameters the same behaviour seen in other scenarios. The interest here is on the semi-hard component structure and on its difference with that of scenario 1. $\bar{N}_{\text{semi-hard}}$ in scenario 2 decreases very fast as the c.m. energy increases, this trend should be compared with that of the semi-hard component in scenario 1: here $\bar{N}_{\text{semi-hard}}$ is an increasing function of c.m. energy in f.p.s. and is constant in different pseudo-rapidity intervals. Accordingly, \bar{n}_c (see Fig. 3) is growing very fast with c.m. energy in scenario 2; it is growing very slowly in f.p.s. and is constant with energy in pseudo-rapidity intervals in scenario 1. These completely different clan structure behaviors when KNO and Feynman scaling are satisfied (scenario 1) and violated (scenario 2) have an interesting interpretation.

Newly created particles of the semi-hard component in scenario 1, being their aggregation power ($1/k_{\text{semi-hard}}$) quite limited and energy independent, give origin to clans whose average number of particles is an energy independent quantity in rapidity intervals (very slowly growing with the extension of the interval) and gently increasing from ≈ 2.5 at 1 TeV to ≈ 3 at 15 TeV in f.p.s. In scenario 2 as the energy increases newly created particles not only continue to aggregate in the existing clans in view of the large value of $1/k_{\text{semi-hard}}$ (if only this fact would occur $\bar{N}_{\text{semi-hard}}$ would be an energy independent quantity, a situation which could be true in scenario 2 for the semi-hard component only asymptotically) but in addition $\bar{N}_{\text{semi-hard}}$ starts to decrease in the TeV region, i.e., the aggregation is now involving clans themselves. Clan aggregation into “super-clans” is an unexpected new phenomenon, which occurs in all rapidity intervals and is less pronounced for pseudo-rapidity intervals of smaller size. For energies much higher than 10 TeV clan aggregation stops ($\bar{N}_{\text{semi-hard}} \approx \text{constant}$) and the new created particles continue to go in the existing super-clans. Scenario 3 confirms for the semi-hard component its main peculiarity to have intermediate properties among those of the semi-hard components in scenarios 1 and 2.

In order to complete our study in Figure 4 we show a comparison for the multiplicity distributions for the small interval $\eta_c = 1$ at c.m. energy 1.8 TeV and c.m. energy 14 TeV. (The figure should be compared also with that one shown in paper I in full phase space).

We notice here how the semi-hard component becomes dominant at 14 TeV c.m.

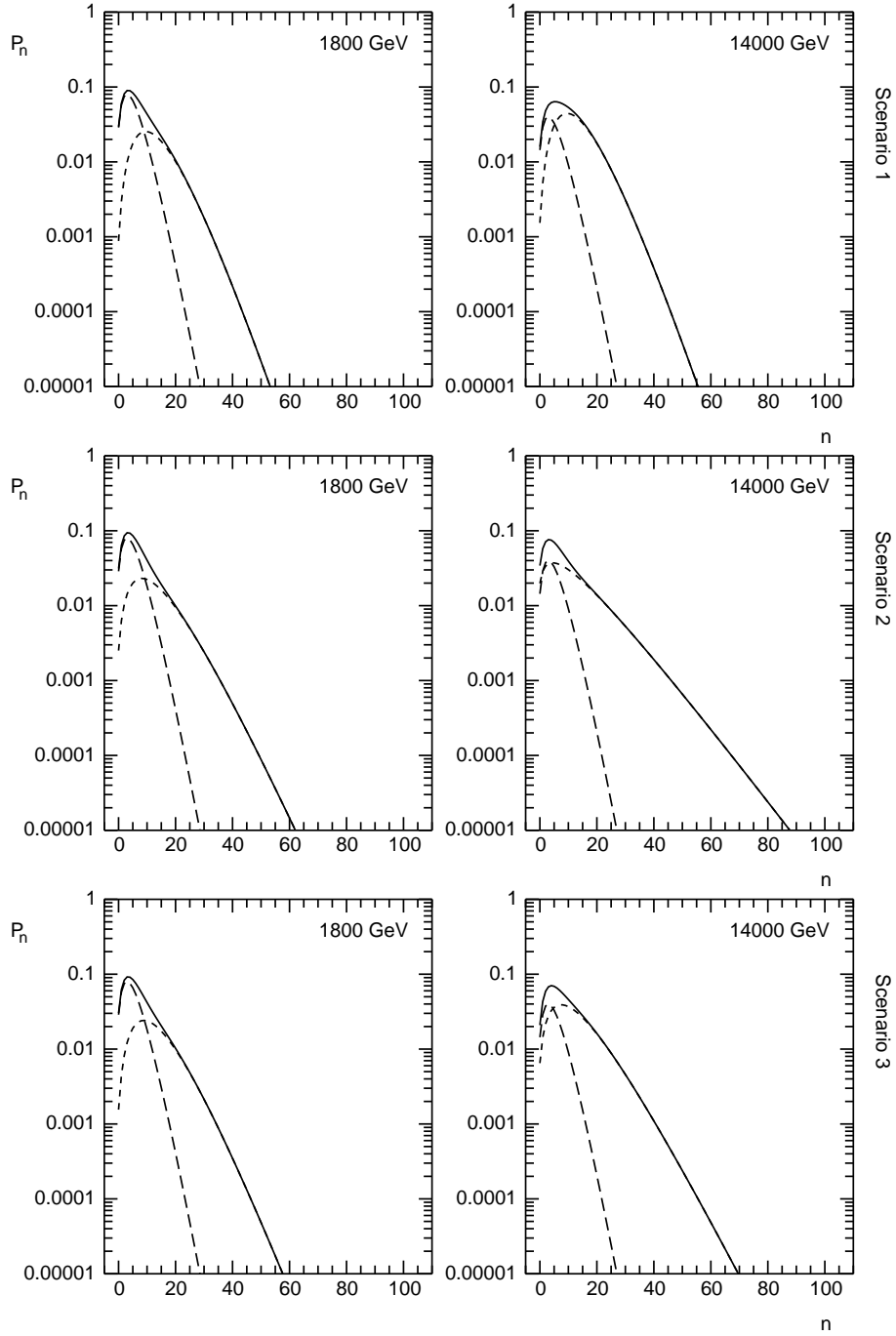


Figure 4: Multiplicity distributions for the pseudo-rapidity interval $|\eta| < 1$, for the three scenarios (top to bottom: scenarios 1, 2, 3) at the c.m. energies of TEVATRON (1.8 TeV) and LHC (14 TeV). Solid line: total distribution; dashed line: soft component; sort-dashed line: semi-hard component.

energy, although in the low multiplicity part of the distributions the soft component is almost as large as the semi-hard one. These graphs confirm the behaviour already seen in f.p.s.

From the analysis of these figures, we conclude that the interesting phenomenon which clan structure analysis allowed to see is not rapidly expanding. This fact points out that in order to distinguish the different scenarios, one should look at $1/k$ parameters and related clan structure analysis, in particular the different behavior between scenarios 1 and 2 is striking. In principle it should be measurable already at the TEVATRON. Scenario 3 is different as its parameters due to the lack of precise QCD calculations on the matter are more flexible and can be adjusted to get close to either one of the other scenarios.

5 Summary

We studied possible scenarios for soft and semi-hard components structures in central hadron-hadron collisions in the TeV region in symmetric pseudo-rapidity intervals. The paper is the natural extension of previous work on hadron-hadron collisions in full phase space and has a twofold motivation. Firstly, in order to understand the dynamics of multiparticle production and related correlations it is important to study their behaviour in regions where the role of conservation laws is negligible. Secondly, future particle accelerators in the TeV energy domain are expected not to be equipped with full acceptance detectors; they will explore limited sectors of full phase space only, unfortunately. Accordingly, the contact of theoretical expectations with experiments in the next decade should be looked for in pseudo-rapidity intervals and not in full phase space. Since we wanted to avoid complications due to the presence of the dip around zero value of pseudo-rapidity variable we considered intervals greater than one unit in rapidity, and in order to be sure that the influence of conservation laws is small we fixed the upper bound to three unit in pseudo-rapidity variable to our intervals on both sides of the origin.

Selected intervals are therefore wide enough (they extend up to six units in rapidity) to allow significant predictions, and chosen in regions not too small and far from the borders of phase space enough to guarantee results not affected by the above mentioned problems. Following paper I and supported by data at lower energies our main assumption has been that soft and semi-hard events are described by Pascal (NB) multiplicity distributions; in addition, the soft event fraction has been taken pseudo-rapidity (interval) independent and varying with center of mass energy only. Total multiplicity distributions are the result of the weighted superposition of the two above mentioned more elementary substructures. Single particle densities develop in our picture an energy independent central plateau for soft and semi-hard components and their difference is limited to the heights of the corresponding two plateaus. The joining to full phase space is taken to be smooth for simplicity leaving more complex situations for future work.

The soft component structure is fully characterized by a k_{soft} Pa(NB)MD parameter which is constant with energy for each pseudo-rapidity interval but varying with its width, i.e., is characterized by Feynman and KNO scaling behaviour.

Three possible scenarios are discussed for the semi-hard component. Scenario 1 has Feynman and KNO scaling as for the soft component, but with different values of the parameters ($1/k_{\text{semi-hard}}$ is energy independent and varies very little with pseudo-rapidity

intervals). In scenario 2 KNO scaling is violated and the width of the total multiplicity distribution grows linearly as $\ln \sqrt{s}$ ($1/k_{\text{semi-hard}}$ is quickly increasing with energy and decreasing with pseudo-rapidity intervals). In scenario 3 the slope of $1/k_{\text{semi-hard}}$ is suggested by QCD: it grows initially with energy but asymptotically (well above the extreme values of the abscissa allowed in figure 1) it tends to a constant value; its increase with energy is not as fast as in scenario 2, but its decrease with pseudo-rapidity intervals quite similar.

In conclusion k_{soft} show wide self-similarity regions and the average number of (soft) clans in a fixed rapidity interval is an energy independent quantity in all three scenarios. In scenario 1, $k_{\text{semi-hard}}$ behaves as k_{soft} but it has a larger value; being the average number of particles in the semi-hard sector larger than in the soft one, clans of the semi-hard component are more numerous than clans of the soft component and have a larger number of particles per clan. In scenario 2 self-similarity appears only as an asymptotic property for the semi-hard component; the average number of clans is decreasing with energy and as the pseudo-rapidity interval decreases but the average number of particles per clan is becoming quite large as the energy increases. Scenario 3 has predictions which are —as expected— intermediate between the previous two.

Of course now the word is to experiments. They will determine which one of the discussed possibilities is closest to the real world. CDF can help in this direction. It is a fact that one should expect the dominance of the semi-hard component structure as the energy increases also in pseudo rapidity intervals, i.e., huge mini-jets production is also here the main characteristic in the new region, as shown explicitly by MDs in a fixed pseudo-rapidity interval at different energies in Figure 4.

In addition the semi-hard component behaviour has a suggestive interpretation in all scenarios in terms of its clan properties. In scenario 1 one notices numerous clan production of nearly equal size as the energy increases in all rapidity intervals. In scenario 2 in all pseudo-rapidity intervals to the aggregation of newly created particles into existing clans follows the aggregation of clans themselves into super-clans (a new species of (mini)-jets) whose average number becomes at asymptotic energies nearly constant. An interesting phenomenon resembling a phase transition in clan production mechanism. Notice that the average number of clan is higher in larger rapidity intervals and its decreasing with energy favours stronger long range correlations.

Scenario 3 leads to predictions which are —as usual— intermediate between the previous two extreme situations but in view of its flexibility can be modified in the two directions as long as QCD will not provide new constraints on our formulae.

6 Acknowledgements

This work was supported in part by M.U.R.S.T. (under Grant 1997). R. U. would like to acknowledge the financial support of the Portuguese Ministry of Science and Technology via the “Sub-Programa Ciência e Tecnologia do 2º Quadro Comunitário de Apoio.”

References

1. A. Giovannini and R. Ugoccioni, “Possible scenarios for soft and semi-hard components structure in central hadron-hadron collisions in the TeV region”, preprint n.

- DFTT 36/98, FISIST/12-98/CENTRA, to appear in Phys. Rev. D.
2. S.G. Matinyan and W.D. Walker, preprint DUKE-TH-98-156; W.D. Walker, talk presented at the XXVIII International Symposium on Multiparticle Dynamics, Delphi, Greece, 6–11 Sept. 1998.
 3. G.J. Alner et al., UA5 Collaboration, Physics Reports 154 (1987) 247.
 4. C. Fuglesang, Multiparticle Dynamics: Festschrift for Léon Van Hove (La Thuile, Italy, 1989) eds. A. Giovannini and W. Kittel, World Scientific, (Singapore, 1990) p. 193.
 5. A. Giovannini and L. Van Hove, Z. Phys. C 30 (1986) 391.
 6. A. Giovannini and L. Van Hove, Acta Phys. Pol. B 19 (1988) 495.
 7. P. Carruthers, Phys. Rev. A 43 (1991) 2632.
 8. G. Calucci and D. Treleani, Nucl. Phys. Proc. Suppl. 71 (1999) 216.